4*H*-SiC photodiodes with micronanostructured receiving surface

© A.V. Afanasev[1], V.V. Zabrodskiy[2], V.A. Ilyin[1], A.V. Serkov[1], V.V. Trushlyakova[1], D.A. Chigirev[1]

[1] St. Petersburg State Electrotechnical University „LETI",
197022 St. Petersburg, Russia
[2] Ioffe Institute,
194021 St. Petersburg, Russia

E-mail: avafanasev@etu.ru

Received February 20, 2025
Revised April 14, 2025
Accepted April 17, 2025

The possibility of using reactive-ion etching (RIE) to form broadband antireflective structures on the surface of photode- tector areas of 4*H*-SiC p^+-n-n^+-photodiodes was investigated. It is shown that during the RIE process utilizing aluminum masks (about ~ 50 nm thick), along thinning of the upper p^+-epilayer, a self-ordered profiled surface with a dominant sharp relief of 600–800 nm is formed due to the effect of micromasking of SiC surface. The formation of this microprofiled surface allows to increase the sensitivity and EQY of 4*H*-SiC photodiodes.

Keywords: 4*H*-SiC, p^+-n-n^+-photodiode, UV band, microprofiling, reactive-ion etching (RIE), responsivity, external quantum yield (EQY)

DOI: 10.61011/SC.2025.01.61074.7633

1. Introduction

Due to its unique combination of properties (large band gap, high breakdown field strength, high thermal conductivity, chemical, thermal and radiation resistance), silicon carbide (SiC) is a semiconductor material for creation of high-performance power, microwave and optoelectronic ultraviolet (UV) devices. It is known that UV SiC photodetectors (FD) based on hexagonal polytypes were one of the first commercially available SiC devices demonstrated as early as in the 1990s. UV SiC photodetectors are currently implemented on the basis of all known types of photodiode structures: Schottky, metal–semiconductor–metal, $p-i-n$, metal–insulator–semiconductor, avalanche photodiode structures both in discrete and matrix design [1]. Nevertheless, investigations of new FD design versions are continued to offer the best combination of low dark currents, high sensitivity (external quantum yield) and quick response [2].

UV sensitivity of FD is defined by the external layer properties (for SiC photodiodes — generally p^+). Primarily by the layer thickness that shall be minimized because absorbed radiation quanta will be mainly recorded in the bulk charge region of FD at a diffusion length distance from the edge of the region [3]. On the other hand, it is known that reflection loss in 4*H*-SiC FD throughout the spectral range of sensitivity (380 nm and lower) is $> 20\,\%$ [1]. Therefore, to increase the efficiency of SiC-FD, along with the decrease in the depth of $p-n$-junction, it is important to create antireflection coatings by forming multilayer antireflection structures [4] or by varying surface morphology. Silicon carbide surface may be modified by short-time electrochemical etching to form a thin porous SiC layer, the presence of which increases the FD efficiency [5,6]. Study [7] investigated the capability of increasing the sensitivity of p^+-n-photodiodes based on 4*H*-SiC by varying the thickness of photo-receiving p^+-regions using the reactive ion plasma etching (RIPE) method, where Ni/Al composition was used as the mask. Note that the effect of nanostructuring of silicon carbide surface during RIPE was not addressed in this study [8]. It was based on two main mechanisms.

The first mechanism was as follows. Etching of a thin (tens of nanometers) aluminum layer at final stages of the process leads to formation of a microisland mask structure with discontinuity. Metal-free surface of SiC is etched at a higher rate than metal leading to microrelief formation.

The second potential relief formation mechanism is as follows. Chemical reactions of plasma components with the surface to be etched produce not only volatile compounds removed from the reaction volume, but also nonvolatile compounds in the form of nanoparticles that may be deposited by plasma onto the SiC surface. For example, during RIPE of SiC in SF_6-O_2-Ar using an aluminum mask, reactions may occur to produce volatile aluminum fluorides and nonvolatile fluorocarbon and aluminum oxide compounds that induce the micronanomasking effect [9]. Optimization of etching parameters and selection of aluminum mask thicknesses make it possible to form high-density arrays of micronanoscale tips on the SiC surface [10]. The presence of such tips can both increase the sensitivity of FD by reducing the reflection coefficient and reduce the sensitivity of FD by increasing the surface recombination centers and diffusion light scattering.

This study that continues study [7] describes the results of investigations of the influence of micronanoscale tips formed by the RIPE method on the surface of photoreceiving pads (PRP) using Al masking coating with various thicknesses on the photovoltaic properties of 4*H*-SiC FD.

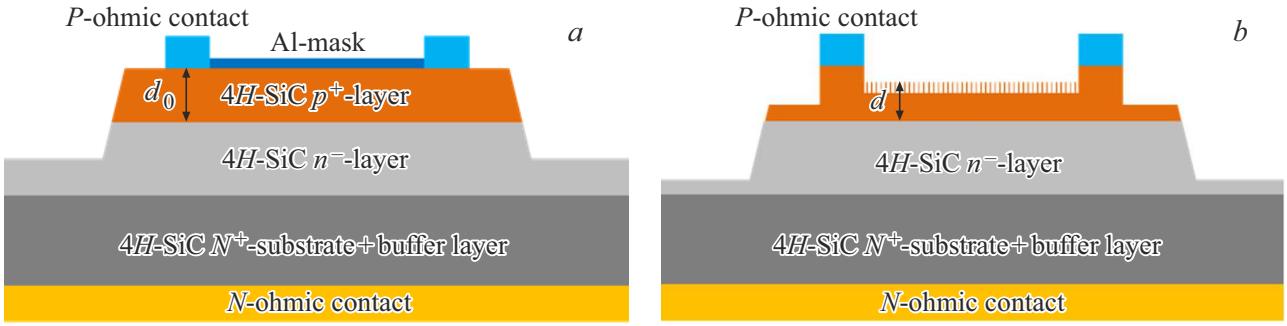

Figure 1. Mesa-epitaxial photodiode 4*H*-SiC-chip: original structure with an aluminum mask (*a*); after RIPE (*b*).

Distribution of SiC FD by groups

Number groups of samples	d_{Al}, nm	RIPE	d, μm
1	0	–	2
2	50	+	1.2
3	100	+	1.2
Study [7]	0	+	1.2

2. Experiment procedure

Photodiodes were made on p^+-n-n^+-epistructures based on 4*H*-SiC formed by the CVD method on the n^+ substrates with a diameter of 100 mm with the following thicknesses and layer doping levels:

– top p^+-layer ($d_0 = 2\,\mu$m, $N_a - N_d > 5 \cdot 10^{19}$ cm^{-3});
– drift n-layer (10 μm, $N_d - N_a < 5 \cdot 10^{14}$ cm^{-3});
– buffer n^+-layer (2 μm, $N_d - N_a > 2 \cdot 10^{18}$ cm^{-3}).

SiC-FD design and manufacturing route were identical to those described in [7] (Figure 1, *a*). After measurement of current-voltage curves and capacitance-voltage curves (Figure 2), the wafer was cut into chips and three groups of samples were formed (see the table). Thin $d_{Al} = 50$ and 100 nm aluminum films were deposited onto PRP of group 2 and 3 samples through the corresponding contact masks (Figure 1, *a*). Selection of such thicknesses, aluminum deposition and RIPE conditions is based on the results of studies [10] that demonstrated formation of SiC micronanotip arrays.

It was taken into account that the grain size of masking metal coating plays an important role in SiC surface modification processes by the RIPE method because etching at the initial RIPE stages is performed between grains, and the smaller the grain size the higher the microtip density per unit area. Therefore to produce thin-film coating with a typical grain size of 30–40 nm, aluminum was deposited by the magnetron sputtering method that was used to form polycrystalline metal films with such grain size.

RIPE of samples from groups 2, 3 that ensured selectivity of etching Al/SiC = 1/15 and etching rate SiC < 0.1 μm/min was implemented on the Caroline-15 ICP unit in the

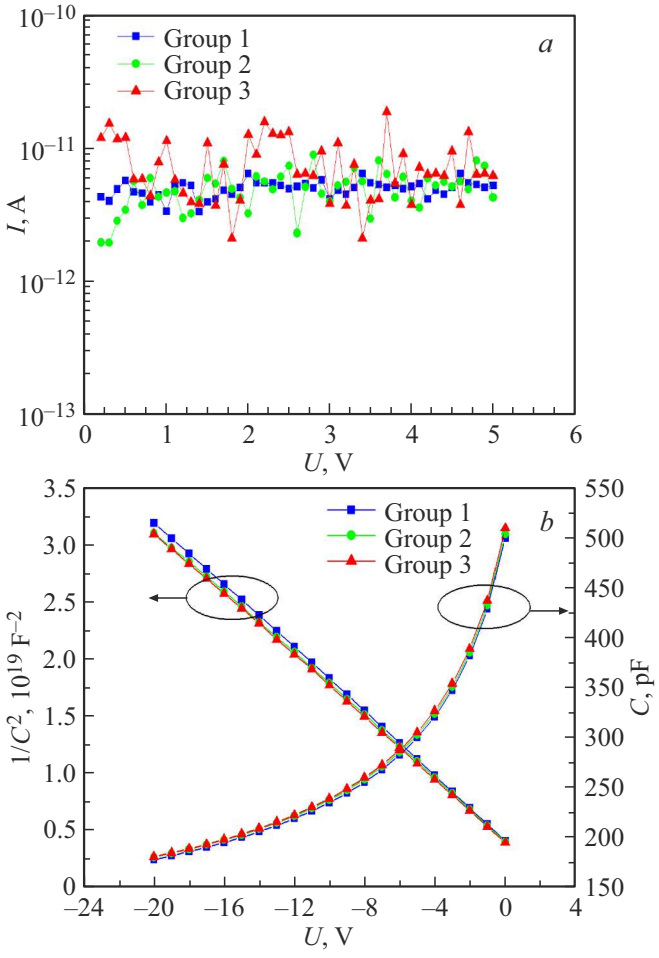

Figure 2. Dark current-voltage curves (*a*) and capacitance-voltage curves ($f = 1$ mHz) (*b*) of 4*H*-SiC-photodiodes (samples of groups 1–3).

following conditions: process temperature — 25 °C; process chamber pressure — 1.2 Pa; medium — SF_6:O_2:Ar (component ratio 4:1:2, respectively); ICP source power — 350 W; HF power — 200 W. Sample etching time was selected so that to ensure the total thickness of the p^+-layer $d = 1-1.2\,\mu$m (Figure 1, *b*), which makes it possible

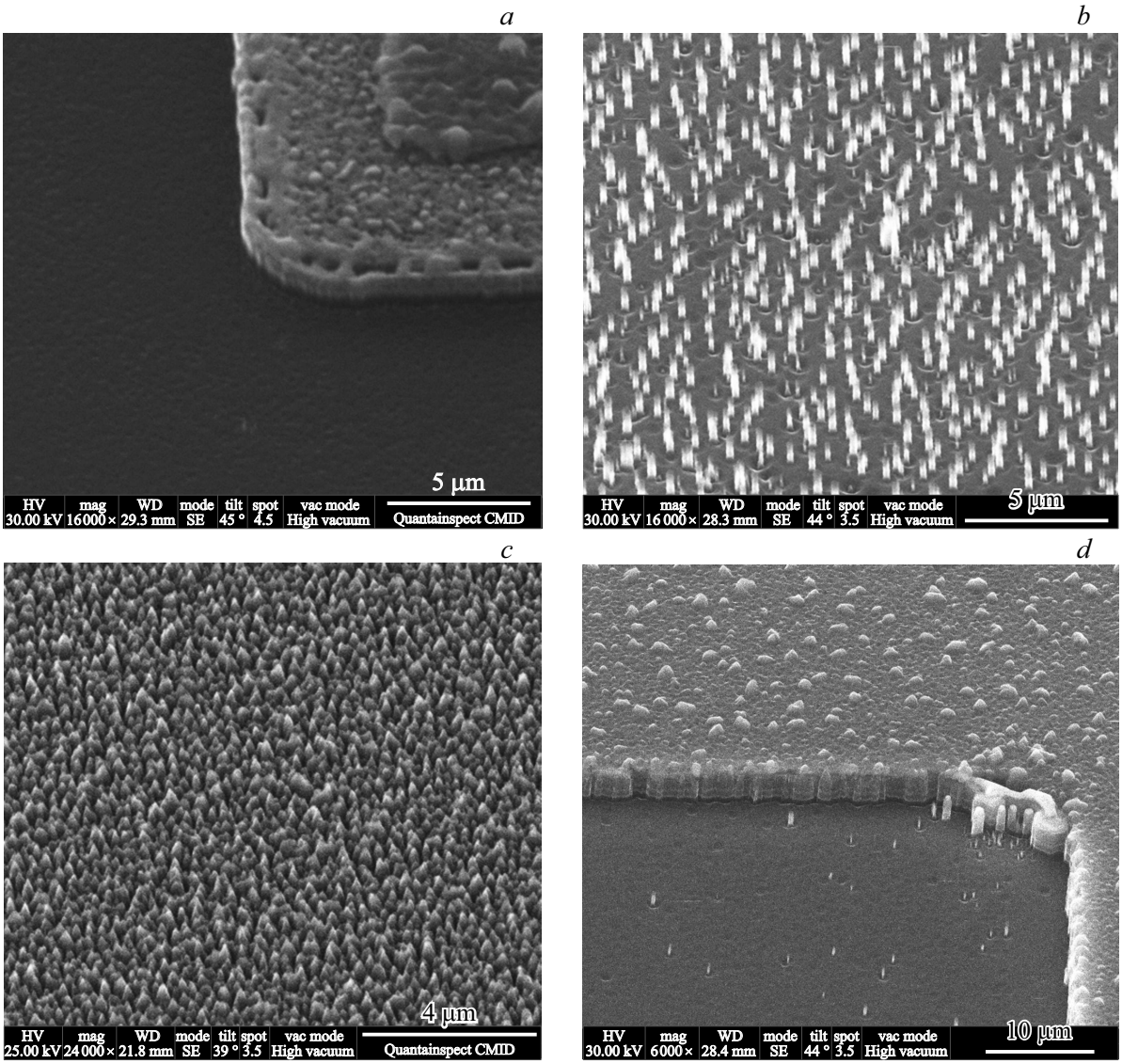

Figure 3. SEM images of photoreceiving pads of SiC-FD: *a* — sample of group 1 (near-electrode region of PRP); *b* — sample of group 2; *c* — sample of group 3; *d* — sample from study [7] (near-electrode regions of PRP).

to compare the characteristics with samples prepared in [7] (see the table).

Sensitivity of samples was studied by the comparison method in short circuit current mode in the wavelength range of 200−400 nm according to the procedure described in [7].

3. Experimental findings

Dark current-voltage curves for all types of samples were measured using the Keithley 6487 picoamperemeter. Reverse currents measured in the range of 0−5 V were 100 pA maximum (Figure, *a*). Capacitance-voltage curves of groups 2 and 3 measured at 1 mHz were plotted in the $C(U)$ coordinates. They almost coincide with the curve of the original sample of group 1 (Figure 2), i. e. areas of the $p-n$-junctions (S_{p-n}) of SiC-FD remained unchanged. Peripheral areas of the top p^+-layer not covered by the Al mask were probably not fully removed (Figure 1, *a*). Doping levels of the*n*-layers for 3 types of samples were determined from the capacitance-voltage curves plotted in the $1/C^2(U)$ coordinates (Figure 2) according to the abrupt asymmetric p^+-n-junction model at $S_{p-n} = 0.1514\,\text{cm}^2$. They were $4-5 \cdot 10^{14}\,\text{cm}^{-3}$, which corresponded to the process settings of original 4*H*-SiC-epistructures.

SiC-FD

PRP was characterized using the SEM method. It follows from Figure 3, *a* that SiC surface of the original sample (group 1) has no any micronanoscale relief. The reference sample in [7] also has no any clear microrelief after RIPE (Figure 3, *d*). At the same time, there is a small amount of microtips on the PRP surface near the ohmic contacts to

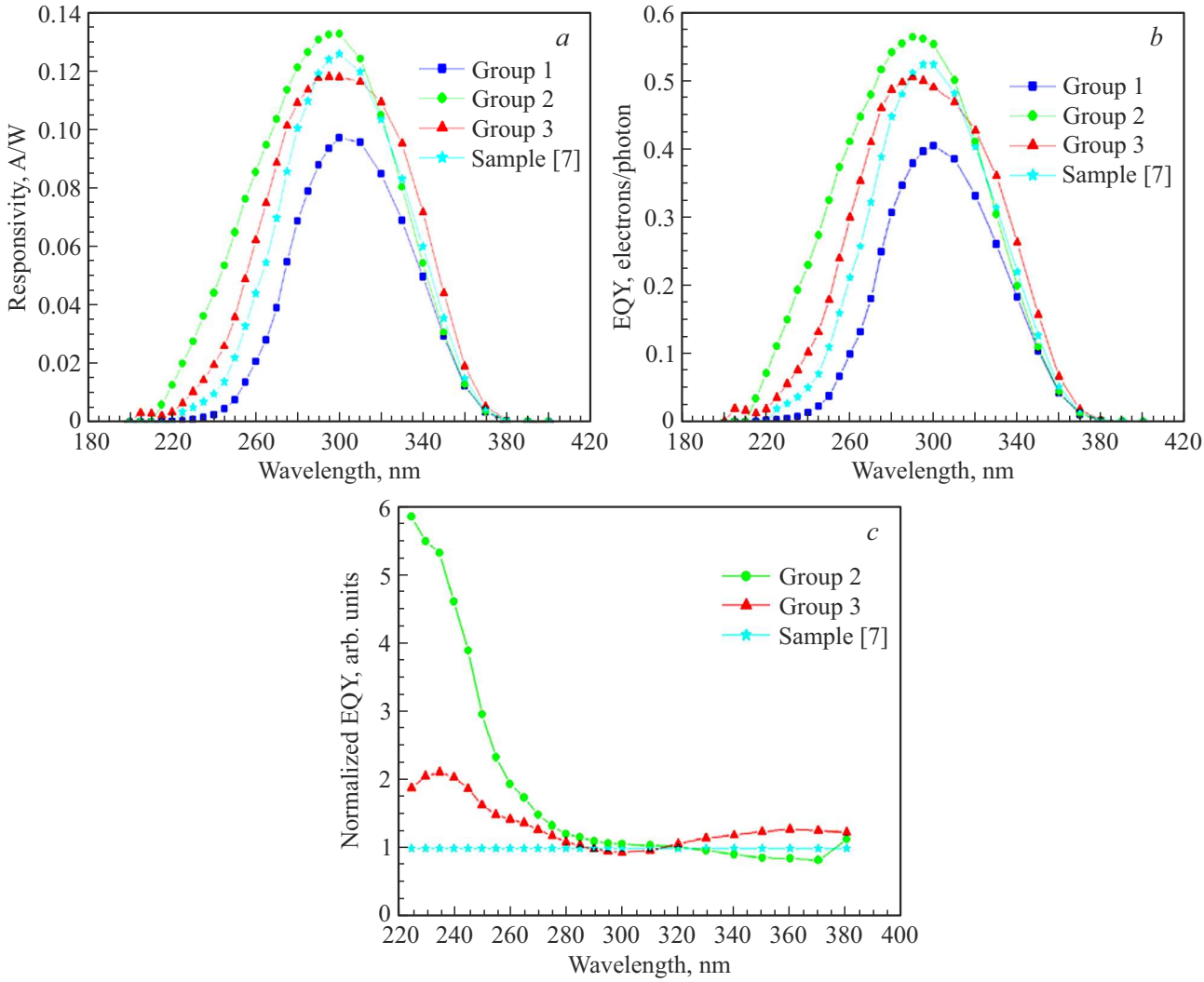

Figure 4. Spectral dependences of sensitivity (a), external quantum yield (b), EQY normalized to sample [7] of 4H-SiC-photodiodes.

the p^+ region made from a multicomponent structure with a top aluminum layer. With the chosen RIPE conditions, this may be probably associated with additional aluminum redeposition and,consequently, by micronanomasking of near-electrode regions.

Figure 3 shows that the density of microtips is much higher for samples from group 3. With the total thickness $d \approx 1.2\,\mu$m of the p^+ layer, PRP of the samples from groups 2 and 3 were characterized by a highly-developed microrelief with microtip heights of $0.6-0.8\,\mu$m and $0.5-0.6\,\mu$m, respectively (Figure 3, b, c). Such microrelief exceeds the wavelength range, in which SiC-FD is used. Therefore, optical properties of the profiled SiC surface will be defined only by its geometry and will not depend on the wavelength.

For spectral measurements, photodiode chips of the samples from groups 1, 2 and 3 were placed in metal-glass casings on subcrystalline boards and welded. Figure 4, a, b shows spectral characteristics of external quantum yield (EQY) of these samples and of the $p-n$-photodiode based on 4H-SiC with the $d \approx 1.2\,\mu$m p^+-layer [7]. In a short-wavelength region (< 280 nm) of spectral characteristics compared with sample [7], sensitivity and EQY are higher for samples from groups 2 and 3. Figure 4, c shows that considerable increase in EQY is observed for samples from group 2. Spectrum broadening and change of the spectral characteristic peak position for samples from this group are probably associated both with a change in microprofile shape on the PRP surface and with a decrease in the thickness of nonprofiled portion of the p^+-region due to a much lower density of microtips compared with the samples of group 3. At the same time, for samples of group 3, where the height of microtips with a higher microtip density was lower by $100-200$ nm compared with group 2, decrease in the sensitivity is observed at the spectral characteristic maximum, and efficiency increases by $20-30\,\%$ in the long-wavelength portion (Figure 4, c). The presence of such surface (Figure 3, c) probably reduces the geometrical

reflection factor leading to an increase in EQY in the wavelength range of 320−380 nm. However, as expected previously, no significant increase in EQY in the short-wavelength region is observed due to an increase in the density of surface recombination centers and diffusion light scattering.

4. Conclusion

RIPE technique using thin (to 100 nm) aluminum films as a masking coating makes it possible to create broadband antireflection layers on the surfaces of photoreceiving regions of 4*H*-SiC p^+-n-n^+ photodiodes. A$\sim$ 50 nm Al mask was found to be the most effective. Thus, an ordered low-density array of SiC microtips with a height of 600−800 nm may be formed in a controlled manner, and simultaneously thinning of the external photoreceiving p^+-region may be provided and the desired microrelief may be formed during RIPE. Both factors contribute to a substantial growth of C-UV sensitivity of SiC-FD. Aluminum masks with a thickness of $\sim$ 100 nm are used in the RIPE method to form high-density arrays of microtips with a height of $<$ 500 nm on the SiC surface and to ensure an increase in the SiC-FD efficiency throughout the spectral range due to a decrease in the geometrical reflection coefficient.

Conflict of interest

The authors declare no conflict of interest.

References

[1] Stephen E. Saddow, Francesco La Via. *Advanced Silicon Carbide Devices and Processing* (IntechOpen, 2015).
[2] Y. Hou, C. Sun, J. Wu, R. Hong, J. Cai, X. Chen, D. Lin, Z. Wu. Electron. Lett., **55**, 216 (2019).
[3] T.V. Blank, Yu.A. Goldberg, E.V. Kalinina, O.V. Konstantinov, A.O Konstantinov, A. Hallen. Pis'ma ZhTF, **27**, 43 (2001). (in Russian).
[4] F. Zhang, W. Yang, H. Huang, X. Chen, Z. Wu, H. Zhu, H. Qi; J. Yao; Z. Fan, J. Shao. Appl. Phys. Lett., **92**, 251102 (2008).
[5] A.V. Afanasyev, V.A. Ilyin, N.M. Korovkina, A.Yu. Savenko. Pis'ma ZhTF, **31**, 1 (2005). (in Russian).
[6] A.V. Afanasiev, V.A. Ilyin. Nano- i mikrosistemnaya tekhnika, **8**, 85 (13). (in Russian).
[7] A.V.Afanasiev, V.V.Zabrodsky, V.A.Ilyin, V.V.Luchinin, A.V.Nikolaev, A.V.Serkov, V.V.Trushlyakova, D.A.Tchigirev. FTP, **56**, 997 (2022). (in Russian).
[8] T. Kimoto, J.A. Cooper. *Fundamentals of silicon carbide technology: growth, characterization, devices and applications* (Singapore, John Wiley & Sons, Inc., 2014).
[9] M. Lazar, H. Vang, P. Brosselard, C. Raynaud, P. Cremillieu, J.-L. Leclercq, A. Descamps, S. Scharnholz, D. Planson. Superlat. Microstr., **40**, 388 (2006).
[10] A.V. Afanasyev, B.V. Ivanov, V.A. Ilyin, A.F. Kardo-Sysoev, M.A. Kuznetsova, V.V. Luchinin. Mater. Sci. Forum, **740**−**742**, 1010 (2013).

Translated by E.Ilinskaya